ISSN 1066-3622, Radiochemistry, 2017, Vol. 59, No. 3, pp. 301–306. © Pleiades Publishing, Inc., 2017.
Published in Russian in Radiokhimiya, 2017, Vol. 59, No. 3, pp. 264–268.

Radioiodination of 3-Amino-2-quinoxalinecarbonitrile 1,4-Dioxide and Its Biological Distribution in Erhlich Ascites Cancer Bearing Mice as a Preclinical Tumor Imaging Agent[1]

I. T. Ibrahim*, S. M. Abdelhalim, M. H. Sanad, and M. A. Motaleb**

Labeled Compounds Department, Hot Laboratories Center, Atomic Energy Authority, P.O. Box 13759, Cairo, Egypt
*e-mail: *ismailtaha_73@yahoo.com, **msanad74@yahoo.com*

Received July 26, 2016

Abstract—3-Amino-2-quinoxalinecarbonitrile 1,4-dioxide (QN) was labeled with ^{125}I, and the biological distribution of the product was studied. ^{125}I-QN was prepared by direct electrophilic substitution reaction using *N*-bromosuccinimide (NBS) as an oxidizing agent. The radiochemical yield of 92% was reached under the following optimum conditions: pH 7, 15 min, 100 μg of QN, and 75 μg of NBS. The labeled QN was stable for up to 12 h post labeling. Biodistribution study of ^{125}I-QN in tumor-bearing mice reflected that it accumulated in tissues with high proliferation rate with preferential accumulation in tumor sites. ^{125}I-QN was incorporated rapidly in the tumor site (T/NT = 4 at 2 h post injection), and then its content slowly decreased, whereas in the other tissues it decreased rapidly. The results obtained encourage the use of ^{123}I-QN as a tumor imaging agent.

Keywords: 3-amino-2-quinoxalinecarbonitrile 1,4-dioxide, iodine-125, labeling, biodistribution, tumor targeting

DOI: 10.1134/S1066362217030146

Quinoxaline and its derivatives are important nitrogen-containing compounds; they exhibit various interesting biological properties and are used in pharmaceutics [1]. The antitumor properties of quinoxaline compounds stimulate synthesis of new derivatives and studies of their biological activity [2]. Analogs of quinoxaline have been investigated as catalyst ligands [3]. Quinoxaline derivatives constitute the building blocks of a wide range of pharmaceuticals exhibiting antibacterial, antifungal, anticancer, and many kinds of activity [4–6]. Quinoxalin-2-ones and quinoxaline-2,3-diones have been reported to show antimicrobial, novel analgesic, anti-inflammatory, and potent antithrombotic activities [7–10]. Study of quinoxaline analogs, such as 2,3-bis(2-pyridyl)quinoxaline, and of their complexes with transition metals is of interest in view of their binding to DNA. Conjugation of biologically active peptides with quinoxaline analogs may lead to new antitumor therapeutic agents. Quinoxaline-1,4-dioxide derivatives seem to have interesting anticancer activities, especially in solid tumor treatment [11]. It was hypothesized that the mechanism of the antitumor effect of quinoxaline derivatives may involve bioreductive alkylation and cleavage of DNA [12, 13]. Radiolabeling of some quinoxaline derivatives with ^{99m}Tc or radioiodine was conducted for imaging or therapeutic purposes, respectively [14]. Auger emitters like ^{125}I were reported to have antitumor effect, especially when introduced into DNA [15]. The high level of cytotoxicity and short-range biological effectiveness of Auger emitters determine their medical applications. Biological effects of Auger emitters are critically dependent on their subcellular (and subnuclear) localization [16–18].

This study was conducted to label 3-amino-2-quinoxalinecarbonitrile 1,4-dioxide with ^{125}I. Factors influencing the radiochemical yield were studied in detail. Biodistribution of ^{125}I-QN in Ehrlich ascites cancer (EAC) bearing mice was studied.

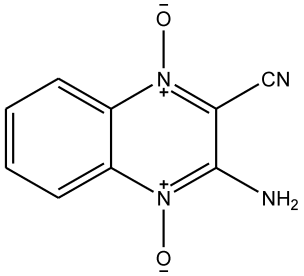

3-Amino-2-quinoxaline-carbonitrile 1,4-dioxide

[1] The text was submitted by the authors in English.

EXPERIMENTAL

Materials. All chemicals and solutions used were of reagent grade. Double-distilled water was used in all experiments for the solution preparation, dilution, and washing purposes. No-carrier-added sodium [^{125}I]iodide (NCA Na^{125}I, 3.7 GBq mL^{-1} in 0.1 N NaOH) for radioiodination was purchased from the Institute of Isotopes, Budapest, Hungary. Quinoxaline was kindly obtained from the Organic Chemistry Chair, Faculty of Science, Damietta University, Egypt. *N*-Bromosuccinimide and sodium metabisulfite were purchased from Aldrich. Methylene chloride, ethyl acetate, and DMF were purchased from the British Drug**.**

Animals. Female Swiss Albino mice weighing 20–25 g were purchased from the Institute of Eye Research, Cairo, Egypt. The animals were kept at constant environmental and nutritional conditions throughout the experimental period at room temperature (22 ± 2°C) with a 12 h on/off light schedule. Standard food and water were allowed to mice all over the experiments. Female mice were used in this study because they are more susceptible to EAC than male mice [19]. Before injection, the drug dose injected to mice was sterilized with a Millipore filter (0.22 μm). The EAC line used in this study was purchased from the National Cancer Institute, Cairo, Egypt.

Synthesis procedure. The radiolabeled compound was prepared by direct electrophilic substitution of QN with carrier-free ^{125}I ($T_{1/2}$ = 60 days) under oxidative conditions in the presence of NBS. To ensure the maximal radiochemical yields, the reaction conditions (oxidizing agent and QN amounts, pH, reaction time) were optimized. Each experiment was repeated five times, and differences in the data were evaluated with unpaired Student's *t*-test. The results are expressed as mean ± SEM. The level of significance was $P < 0.05$.

^{125}I-QN was prepared by adding a solution of QN in DMF (200 μg in 100 μL) to a solution of NBS in 95% ethanol (50 μg in 10 μL). The pH was adjusted to 7 by adding 150 μL of a phosphate buffer (pH 7). Then, 10 μL of the ^{125}I solution (74 kBq) was added, and the reaction was performed for 15 min at ambient temperature. The reaction was stopped by adding a solution of sodium metabisulfite in ethanol (100 μg in 15 μL).

Chromatographic analysis. *TLC.* Analysis was performed using silica gel coated aluminum sheets (20 × 20 cm). The sheet was cut into strips 1 cm wide and 13 cm long. The sample was spotted at a distance of 2 cm above the edge. The solvent used for developing was methylene chloride–ethyl acetate (2 : 1 v/v).

Paper electrophoresis. On a Whatman paper sheet (2 × 47 cm), 1–2 μL of the reaction mixture was placed 12 cm above the lower edge. The solution was allowed to evaporate spontaneously. Electrophoresis was carried out for 90 min at a voltage of 300 V using 0.5 M phosphate buffer (pH 7.6) as electrolyte. After complete development, the paper was removed, dried, and cut into strips 2 cm wide. Each strip was counted in a well-type γ-counter.

The radiochemical yield was estimated as the percent ratio of the radioactivity of ^{125}I-QN to the total activity.

Docking study. This technique consists in direct molecular modeling of the system of the ligand and target protein with the known 3D structure. The method is used for detailed estimation of intermolecular interactions between the ligand and the target protein. An automated docking study was carried out using the crystal structure of inhibitor topotecan/topoisomerase I complex obtained from the protein data bank website (1SC7 code, resolution 2.0 Å). This regularized protein complex structure was used for determining the enzyme active site. The performance of the docking method on topoisomerase I inhibitors was evaluated and validated by redocking the crystalline ligand, topotecan; the RMSD value obtained was 0.00421 [20]. Docking was carried out for the tested compound. In the flexible ligand–rigid enzyme docking, the enzyme was represented by six potential energy maps, namely, electrostatic, hydrogen bond, hydrophobic, and three van der Waals maps. The predicted binding energy of the new compound is –29.45 kcal mol^{-1} [21].

Tumor transplantation in mice. EAC cell is a model for studying the biological behavior of malignant tumors and drugs assumed to produce effect at these sites [14]. EAC was maintained in female mice via weekly intraperitoneal (IP) transplantation of 2.5 × 10^6 tumor cells per mouse. EAC cells were obtained by needle aspiration under aseptic condition. The ascitic fluid was diluted with sterile saline so that 0.1 mL contained 2.5 × 10^6 cells counted microscopically using a hemocytometer. About 0.2 mL of the solution was then injected intraperitoneally to produce ascites and intramuscularly in the right thigh to produce solid tumor

with the left thigh kept as control. The animals were maintained for 10–15 days until the tumor development became apparent [22].

Biodistribution of ^{125}I-QN in mice. In-vivo biodistribution studies were performed using 4 groups of normal mice, of ascites-bearing mice, and of solid timor bearing mice. Each group consisted of five mice. Each animal was injected in the tail vein with 0.2 mL of a solution containing 2 μCi (74 kBq) of ^{125}I-QN. The mice were kept in metabolic cages for the required time. Each mouse was weighed and then anaesthetized with ether. Samples of fresh blood, bones (femoral bone) and muscles (left thigh muscle) were collected in preweighed vials. For ascites-bearing mice, ascitic fluid was withdrawn with a 20-cm plastic syringe. For solid tumor bearing mice, the right and left legs were removed and weighed. The weight of blood, bone, and muscles was assumed to be 7, 10, and 40% of the total body weight, respectively [23]**.** Organs or tissues of interest were removed, weighed, and counted on a γ-counter. Correction was made for the background radiation and physical decay during the experiment [24]. The activity was measured in counts per minute. The uptake was calculated in percents of the injected dose per gram of the tissue or organ (% ID/g). All experiments were performed in compliance with the rules of animal ethics sited by Labeled Compounds Department, Hot Laboratories Center, Egyptian Atomic Energy Authority.

RESULTS AND DISCUSSION

Chromatographic analysis. TLC analysis showed that ^{125}I-QN moved with the mobile phase (R_f = 0.8–1), whereas free iodide remained near the point of spotting (R_f = 0–0.1).

Electrophoresis experiments showed that free radioiodide moved to a distance of 12–16 cm away from the spotting point, whereas ^{125}I-QN moved by no more than 6 cm (Fig. 1).

Factors influencing the radiochemical yield of ^{125}I-QN. *NBS amount.* As seen from Fig. 2, 75 μg is the optimum amount of oxidizing agent required to obtain the maximal radiochemical yield (92.1%). Lower amounts of NBS are apparently insufficient to oxidize all iodide ions to iodonium ions; e.g., with 10 μg of NBS the free iodide content was 23.1%. As the NBS amount was increased over 75 μg, the radiochemical yield did not change significantly.

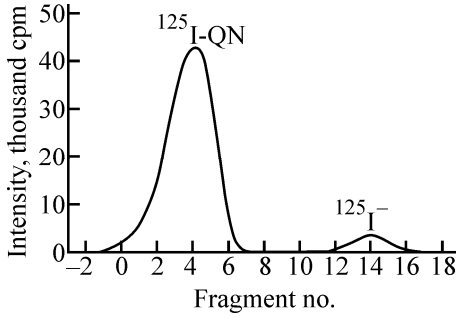

Fig. 1. Paper electrophoresis for ^{125}I-QN and free iodide.

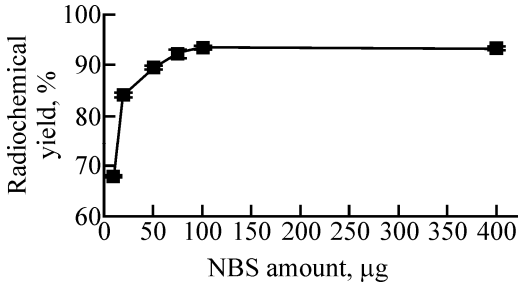

Fig. 2. Influence of the NBS amount on the radiochemical yield of ^{125}I-QN.

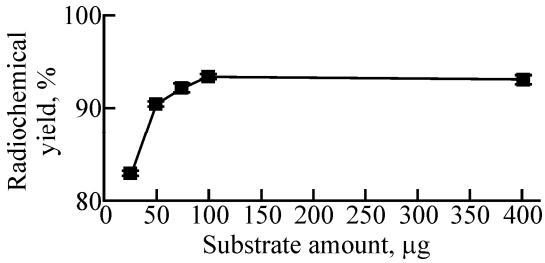

Fig. 3. Influence of the QN amount on the radiochemical yield of ^{125}I-QN.

QN amount. The radiochemical yield increased with increasing QN amount, reaching a maximum (92.1%) at 75 μg of QN. Apparently, lower QN amounts were insufficient for binding all the generated iodonium ions. For example, with 25 μg of QN the radiochemical yield was 82.8%. As the QN amount was increased over 75 μg, the yield did not change noticeably (Fig. 3).

pH. Labeling was performed with high yield at neutral pH 7. At higher or lower pH values, the yield decreased (Fig. 4).

Reaction time. Figure 5 shows the relationship between the reaction time and the yield of ^{125}I-QN. The reaction is fast because of high reactivity of QN. The 91.7% yield was reached in 10 min. As the reac-

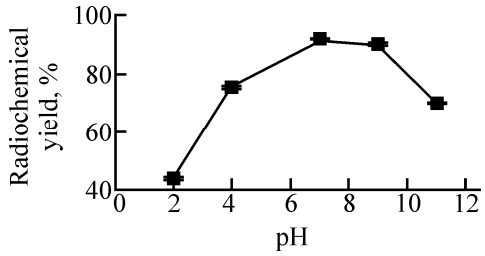

Fig. 4. Influence of pH of the reaction medium on the radiochemical yield of ^{125}I-QN.

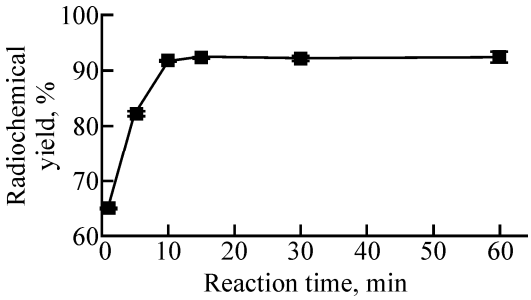

Fig. 5. Influence of the reaction time on the radiochemical yield of ^{125}I-QN.

tion time was increased to 60 min, the yield did not appreciably increase further.

In vitro stability of ^{125}I-QN. It was found that ^{125}I-QN was stable for up to 24 h post labeling.

Docking. The docking position of the tested compound is shown in Fig. 6. Docking furnishes useful information for understanding the structural features of the target and the necessary chemical features of the ligand. The predicted binding mode of our compound showed the formation of two H bonds at distances of 2.07 and 2.15 Å with Arg 364. There are also π–π interactions with DA113, DT10, and TGP11 and strong π–cation interactions with the same fragments. These interactions account for the high binding energy of our compound and the good biological activity.

Biodistribution of ^{125}I-QN in mice. *Normal mice.* Biodistribution study of ^{125}I-QN in normal mice showed that ^{125}I-QN was distributed in blood, liver, stomach, heart, and intestine at 15 min post injection. After 60 min, the ^{125}I-QN uptake significantly decreased in blood and heart but significantly increased in liver, bones, muscles, stomach, and thyroid. At 120 and 240 min post injection, the majority of tissues showed significant decrease in the ^{125}I-QN uptake. Thyroid gland showed significant increase in the ^{125}I-QN uptake at 120 min post injection (Table 1).

Ascites-bearing mice. The results of these experiments showed that the organs of highest uptake at 15 min post injection were blood, liver, heart, and stomach. Table 2 shows that the ^{125}I-QN concentration at 15 min post injection was the lowest in thyroid, muscles, and spleen. The ^{125}I-QN uptake in ascitic fluid was rapid and reached 2.8% ID/mL at 15 min post injection, and at 60 and 120 min it reached approximately 5.6 and 5.3% ID/mL, respectively. At 240 min post injection, the ^{125}I-QN uptake in ascitic fluid did not change significantly relative to the previous value.

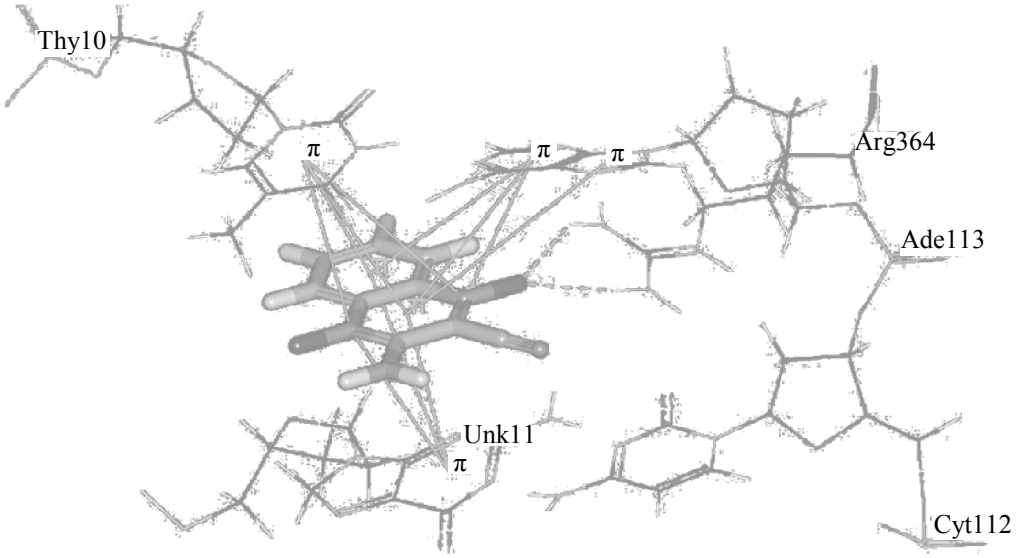

Fig. 6. Quinoxaline docking.

Table 1. Biodistribution of ^{125}I-QN in normal mice (% ID/g) at different times post injection[a]

Organ or body fluid	15 min	60 min	120 min	240 min
Blood	16.1 ± 0.03	11.8 ± 0.09*	4.4 ± 0.11*	1.5 ± 0.07*
Bones	1.16 ± 0.23	2.5 ± 0.15*	0.9 ± 0.13*	0.3 ± 0.01*
Muscles	1.2 ± 0.02	2.51 ± 0.13*	1.7 ± 0.08*	0.4 ± 0.03*
Liver	8.9 ± 0.1	11.2 ± 0.08*	5.1 ± 0.04*	1.5 ± 0.01*
Lungs	2.6 ± 0.05	4.9 ± 0.04*	2.3 ± 0.14*	0.6 ± 0.05*
Heart	5.7 ± 0.2	3.3 ± 0.12*	1.3 ± 0.12*	0.5 ± 0.07*
Stomach	7.5 ± 0.2	12.7 ± 0.19	5.6 ± 0.16*	2.5 ± 0.07*
Intestine	5.3 ± 0.1	7.5 ± 0.28*	4.0 ± 0.1*	1.4 ± 0.11*
Kidneys	2.6 ± 0.16	5.6 ± 0.22*	2.6 ± 0.08*	0.5 ± 0.01*
Spleen	1.2 ± 0.06	2.76 ± 0.1*	1.4 ± 0.1	0.3 ± 0.03*
Thyroid	2.6 ± 0.16	4.4 ± 0.13*	8.7 ± 0.17*	8.5 ± 0.13*

[a] Values are given as mean ± SEM, $n = 5$. The values significantly differing from the previous values in accordance with unpaired Student's t-test ($P < 0.05$) are marked with an asterisk. The same for Tables 2 and 3.

Table 2. Biodistribution of ^{125}I-QN in ascites-bearing mice (% ID/g) at different times post injection

Organ or body fluid	15 min	60 min	120 min	240 min
Blood	11.7 ± 0.3	11.4 ± 0.35*	3.1 ± 0.04*	1.4 ± 0.06*
Bones	1.38 ± 0.08	3.3 ± 0.09*	1.7 ± 0.1*	0.2 ± 0.01*
Muscles	2.5 ± 0.09	3.0 ± 0.05*	1.5 ± 0.04*	0.6 ± 0.01*
Liver	9.6 ± 0.06	10.7 ± 0.16*	3.5 ± 0.12*	1.5 ± 0.06*
Lungs	2.5 ± 0.3	3.2 ± 0.09*	1.6 ± 0.09*	0.3 ± 0.01*
Heart	6.9 ± 0.12	3.1 ± 0.06*	1.4 ± 0.05*	0.4 ± 0.02*
Stomach	6.8 ± 0.1	9.9 ± 0.18*	4.2 ± 0.12*	1.4 ± 0.17*
Intestine	5.2 ± 0.19	7.4 ± 0.15*	4.1 ± 0.06*	1.3 ± 0.04*
Kidneys	2.5 ± 0.1	5.2 ± 0.17*	2.4 ± 0.08*	0.4 ± 0.07*
Spleen	1.3 ± 0.14	1.9 ± 0.05*	1.3 ± 0.14*	0.3 ± 0.1*
Thyroid	1.4 ± 0.12	4.4 ± 0.07*	8.6 ± 0.17*	8.7 ± 0.2
Ascitic fluid	2.84 ± 0.12	5.6 ± 0.11*	5.3 ± 0.08	5.1 ± 0.07*

Table 3. Biodistribution of ^{125}I-QN in solid tumor bearing mice (% ID/g) at different times post injection

Organ or body fluid	15 min	60 min	120 min	240 min
Blood	13.9 ± 0.3	10.7 ± 0.24*	3.4 ± 0.1*	1.4 ± 0.09*
Bones	1.3 ± 0.03	2.4 ± 0.1*	1.4 ± 0.1*	0.4 ± 0.04*
Liver	8.3 ± 0.13	10.3 ± 0.17*	4.4 ± 0.14*	0.6 ± 0.01*
Lungs	2.5 ± 0.05	4.1 ± 0.2*	1.8 ± 0.17*	0.3 ± 0.02*
Heart	4.5 ± 0.1	3.0 ± 0.11*	1.2 ± 0.04*	0.6 ± 0.06
Stomach	8.2 ± 0.14	11.0 ± 0.18*	5.3 ± 0.15*	2.4 ± 0.07*
Intestine	4.9 ± 0.13	6.3 ± 0.13*	4.3 ± 0.15*	1.4 ± 0.09
Kidneys	2.3 ± 0.16	5.4 ± 0.15*	3.2 ± 0.16*	1.35±0.09*
Spleen	1.3 ± 0.1	2.2 ± 0.08*	1.2 ± 0.09*	0.3 ± 0.06*
Thyroid	2.3 ± 0.07	4.5 ± 0.18*	6.5 ± 0.14*	6.9 ± 0.05
Normal muscle	1.3 ± 0.1	2.2 ± 0.08*	1.4 ± 0.1*	0.5 ± 0.07*
Tumor muscle	2.6 ± 0.17	5.4 ± 0.1*	5.7 ± 0.2	4.3 ± 0.3

At 60 min post injection, the uptake in stomach and liver significantly increased, and in blood and heart it decreased. At 120 min post injection, the majority of organs showed significant decline in the ^{125}I-QN uptake. Only in ascitic fluid and thyroid there was a significant increase in the uptake at 120 min post injection. The excretion was mainly through kidneys via urine and in part through GIT with feces. At 240 min

post injection, the majority of organs showed significant decrease in the ^{125}I-QN uptake.

Solid tumor bearing mice. Table 3 shows that in solid tumor bearing mice ^{125}I-QN rapidly distributed in blood, liver, stomach, and heart at 15 min post injection. The inoculated muscle uptake at 15 min post injection was about 2.6% and significantly increased at 60 and 120 min post injection. At 60 min post injection, stomach, intestine, and kidneys showed a significant increase in the ^{125}I-QN uptake, while most of others tissues showed a significant decrease. The majority of organs show a significant decrease in the ^{125}I-QN uptake at 240 min post injection.

Thus, QN was labeled with radioiodine with 92% yield. ^{125}I-QN was stable in vitro for up to 24 h post labeling. Biodistribution of ^{125}I-QN in tumor-bearing mice revealed that it distributed rapidly to ascites or solid tumor site, with the uptake increasing with time. On the other hand, the blood and liver uptake declined rapidly. The results obtained suggest that ^{123}I-QN is a promising radiopharmaceutical for tumor imaging.

REFERENCES

1. Brown, H.C. et al., *Determination of Organic Structures by Physical Methods*, Baude, E.A. and Nachod, F.C., Eds., New York: Academic, 1955.
2. Xiang-Hong Wu, Gang Liu, et al., *Mol. Diver.,* 2004, vol. 8, no. 2, pp. 165–147.
3. Renault, J., Baron, M., Mailliet, P., et al., *Eur. J. Med. Chem*., 1981, vol. 16, no. 6, pp. 545–550.
4. Wu, X. and Gorden, A.E.V., *J. Org. Chem.,* 2007, vol. 72, no. 23, pp. 8691–8699.
5. Heravi, M.M., *ARKIVOC*, 2006, vol. 2006, pp. 16–22.
6. Chen, B., Su, B., and Chen, S., *Biochem. Pharmacol*., 2009, vol. 77, no. 12, pp. 1787–1794.
7. Greenhough, A., Smartt, H.J.M., Moore, A.E., et al., *Carcinogenesis*, 2009, vol. 30, no. 3, pp. 377–386.
8. Brown, J.R. et al., *J. Clin. Oncol*., 2005, vol. 23, pp. 2840–2855.
9. Harris, R.E., Chlebowski, R.T., Jackson, R.D., et al., *Cancer Res*., 2003, vol. 63, pp. 6096–6101.
10. Harris, R.E., Namboodiri, K., Stellman, S.D., and Wynder, E.L., *Prev. Med*., 1995, vol. 24, pp. 119–120.
11. Harris, R.E., Namboodiri, K.K., and Farrar, W.B., *Epidemiology*, 1996, vol. 7, pp. 203–205.
12. Mazhar, D., Ang, R., and Waxman, J., *Br. J. Cancer*, 2006, vol. 94, pp. 346–350.
13. Giardiello, F.M. et al., *Gastroenterology*, 2004, vol. 126, pp. 425–431.
14. Su, B., Landini, S., Davis, D.D., and Brueggemeier, R.W., *J. Med. Chem*., 2007, vol. 50, pp. 1635–1644.
15. Kassis, A.I., *J. Nucl. Med*., 2003, vol. 44, no. 9, pp. 1479–1481.
16. El-Azony, K.M., *J. Radioanal. Nucl. Chem*., 2010, vol. 285, pp. 315–320.
17. Motaleb, M.A., Moustapha, M.E., and Ibrahim, I.T., *J. Radioanal. Nucl. Chem*., 2011, vol. 289, no. 1, pp. 239–245.
18. Petzold, G. and Coenen, H.H., *J. Label. Compd. Radiopharm*., 1981, vol. 18, p. 139.
19. Knust, E.J., Dutschka, K., and Machulla, H.J., *J. Radioanal. Nucl. Chem. Lett*., 1990, vol. 144, p. 107.
20. Singh, S.K., Ruchelman, A.L., Li, T.K., et al., *J. Med. Chem*., 2003, vol. 46, p. 2254.
21. Nagarajan, M., Morrell, A., Ioanoviciu, A., et al., *J. Med. Chem*., 2006, vol. 49, p. 6283.
22. Saccavini, J.C. and Bruneau, C., *IAEA CN 4519*, 1984, p. 153.
23. Tolmachev, V., Bruskin, A., Sivaev, I., et al., *Radiochim. Acta*, 2002, vol. 90, pp. 229–235.
24. Motaleb, M.A., El-Kolaly, M.T., Rashed, H.M., and Abd El-Bary, A., *J. Radioanal. Nucl. Chem*., 2011, vol. 289, pp. 915–921.